Supramolecular Chemistry
Publication details, including instructions for authors and subscription information:
http://www.informaworld.com/smpp/title~content=t713649759

Design of supramolecular β-sheet forming β-turns containing aromatic rings and non-coded α-aminoisobutyric acid and the formation of flat fibrillar structures through self-assembly

Sudeshna Kar[a]; Arpita Dutta[a]; Michael G. B. Drew[b]; Pradyot Koley[a]; Animesh Pramanik[a]
[a] Department of Chemistry, University of Calcutta, Kolkata, India [b] School of Chemistry, The University of Reading, Whiteknights, Reading, UK

To cite this Article Kar, Sudeshna , Dutta, Arpita , Drew, Michael G. B. , Koley, Pradyot and Pramanik, Animesh(2009) 'Design of supramolecular β-sheet forming β-turns containing aromatic rings and non-coded α-aminoisobutyric acid and the formation of flat fibrillar structures through self-assembly', Supramolecular Chemistry, 21: 8, 681 — 690
To link to this Article: DOI: 10.1080/10610270802709378
URL: http://dx.doi.org/10.1080/10610270802709378

Supramolecular Chemistry
Vol. 21, No. 8, December 2009, 681–690

Taylor & Francis
Taylor & Francis Group

Design of supramolecular β-sheet forming β-turns containing aromatic rings and non-coded α-aminoisobutyric acid and the formation of flat fibrillar structures through self-assembly

Sudeshna Kar[a], Arpita Dutta[a], Michael G.B. Drew[b]*, Pradyot Koley[a] and Animesh Pramanik[a]*

[a]*Department of Chemistry, University of Calcutta, Kolkata, India;* [b]*School of Chemistry, The University of Reading, Whiteknights, Reading, UK*

(*Received 15 September 2008; final version received 10 December 2008*)

Single crystal X-ray diffraction studies show that the three designed tripeptides Boc-Leu-Aib-*m*-NA-NO_2 (**I**), Boc-Phe-Aib-*m*-NA-NO_2 (**II**) and Boc-Pro-Aib-*m*-ABA-OMe (**III**) (Aib, α-aminoisobutyric acid; *m*-NA, *m*-nitroaniline; *m*-ABA, *m*-aminobenzoic acid; Boc, *t*-butyloxycarbonyl) containing aromatic rings in the backbones adopt β-turn structures that are self-assembled through intermolecular hydrogen bonds and van der Waals interactions to create layers of β-sheets. Solvent-dependent NMR titration and CD studies show that the β-turn structures of the peptides also exist in the solution phase. The field emission scanning electron microscopic and transmission electron microscopic images of the peptides in the solid state reveal fibrillar structures of flat morphology that are formed through β-sheet mediated self-assembly of the preorganised β-turn building blocks.

Keywords: peptide; α-aminoisobutyric acid; β-turn; β-sheets; flat morphology

Introduction

The design and synthesis of appropriate peptide subunits for desired supramolecular architecture is an important area of current research. Supramolecular helices (*1*, *2*) and β-sheets (*3*) are the most common supramolecular architectures derived from peptides through self-assembly. Supramolecular β-sheets have many potential applications in material (*4–7*) as well as in biological sciences (*8–11*). Amyloid fibril forming β-sheets are the causative factors of many neurodegenerative diseases (*12*, *13*). It has been observed that a β-turn subunit can either form a supramolecular β-sheet or form a supramolecular helix through self-assembly (*14–16*). In this paper, we are interested in designing small synthetic peptides that exhibit β-turns, and have the potential to form supramolecular β-sheets through molecular self-assembly.

In the present report, the three model tripeptides Boc-Leu-Aib-*m*-NA-NO_2 (**I**), Boc-Phe-Aib-*m*-NA-NO_2 (**II**) and Boc-Pro-Aib-*m*-ABA-OMe (**III**) (Aib, α-aminoisobutyric acid; *m*-NA, *m*-nitroaniline; *m*-ABA, *m*-aminobenzoic acid; Boc, *t*-butyloxycarbonyl) with a centrally placed non-coded amino acid Aib have been chosen (Figure 1). Since short aromatic peptides have the ability to form β-sheet-mediated amyloid fibrils (*17*), peptides **I**–**III** have been designed to incorporate *m*-NA and *m*-ABA, which are equivalent to the rigid γ-aminobutyric acid with an all-*trans* extended configuration. Generally, conformationally restricted Aib is a β-sheet breaker and highly helicogenic. Therefore, tripeptides **I**–**III** with a centrally positioned Aib(2) are expected to adopt β-turn structures (*3*, *18–24*). It will be interesting to know whether the incorporation of *m*-NA or *m*-ABA assists or disrupts the creation of the β-turn structure. There are examples of constrained cyclic peptides in which *o*-substituted benzenes have been inserted to mimic the turn region of the neurotrophin, a nerve growth factor (*25*). Peptides **I**–**III** will be three acyclic analogues of these cyclic peptides if they adopt β-turn structures. The present study will also reveal the influence of aromatic rings in self-assembly, especially in the formation of supramolecular β-sheet. Peptides **I**–**III** were synthesised using conventional solution-phase methodology and their solid-state structures and crystal packing were determined by X-ray diffraction analysis. Their conformations in the solution phase were probed by CD and NMR studies. Field emission scanning electron microscopy (FE-SEM) and transmission electron microscopy (TEM) have been employed to investigate the morphological properties of the peptides in the solid state.

Results and discussion

Peptide conformations and packing in the solid state

Peptide Boc-Leu-Aib-*m*-NA-NO_2 (**I**) crystallises with two molecules in the crystallographic asymmetric unit designated as **A** and **B**. In both molecules, the chirality at C(4) is *S*. The crystal structure of peptide **IA** reveals a type II′ β-turn structure with Leu(1) and Aib(2) occupying

*Corresponding authors. Email: animesh_in2001@yahoo.co.in; m.g.b.drew@reading.ac.uk

ISSN 1061-0278 print/ISSN 1029-0478 online

DOI: 10.1080/10610270802709378
http://www.informaworld.com

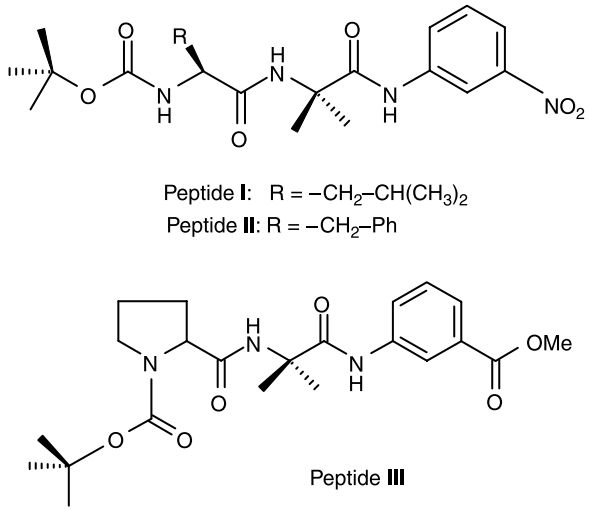

Figure 1. Schematic representation of peptides **I**–**III**.

the $i+1$ and $i+2$ positions, respectively (Figure 2). The torsion angles at Leu(1) and Aib(2) are found to be $\varphi_1 = 50.3°$, $\psi_1 = -132.7(2)°$ and $\varphi_2 = -61.1(3)°$, $\psi_2 = -30.0(3)°$, respectively (Table 1), which are deviated from the ideal values for a type II′ β-turn $\varphi_1 = 60°$, $\psi_1 = -120°$ and $\varphi_2 = -80°$, $\psi_2 = 0°$ (*26*). The corresponding torsion angles in **IB** are $\varphi_1 = -60.6(3)°$, $\psi_1 = 147.6(2)°$ and $\varphi_2 = 58.4(3)°$, $\psi_2 = 32.1(3)°$, respectively (Table 1), indicating a type II β-turn structure. Interestingly, the change in signs of the torsion angles reflect the fact that the packing of the molecule almost conforms to space group $P2_1/a$ with the major difference that C(4) has *S* chirality in both molecules. Peptides **IA** and **IB** are therefore two conformational isomers. The conformational isomorphism of β-turns has been observed in HIV protease (*27*). The β-turn conformations of **IA** and **IB** possess weak intramolecular $4 \rightarrow 1$ hydrogen bonds between *m*-NA—NH and Boc-CO with N9(A)–O2(A) and N9(B)–O2(B) distances as 3.47(1) and 3.56(1) Å, respectively (Table 2; Figure 2).

Peptide Boc-Phe-Aib-*m*-NA-NO_2 (**II**) crystallises in a centrosymmetric space group with one molecule in the asymmetric unit. Inspection of the torsion angles of the corner residues Phe(1) and Aib(2) ($\varphi_1 = -57.9(3)°$, $\psi_1 = 143.5(2)°$ and $\varphi_2 = 70.3(3)°$, $\psi_2 = 13.2(3)°$) reveals that peptide **II** adopts a type II β-turn structure (Figure 3; Table 1), stabilised by a weak intramolecular $4 \rightarrow 1$ hydrogen bond between *m*-NA—NH and Boc-CO with an N9–O2 distance as 3.34(1) Å (Table 2).

The crystal structure of the peptide Boc-Pro-Aib-*m*-ABA-OMe (**III**) is determined in the non-centrosymmetric space group $P2_1$, with C(4) chosen to have *S* chirality. The structure reveals a β-turn structure similar to that found in peptides **I** and **II** with Pro(1) and Aib(2) occupying the $i+1$ and $i+2$ positions, respectively (Figure 4). The torsion angles at the corner residues Pro(1) and Aib(2) are found to be as $\varphi_1 = -48.4(3)°$, $\psi_1 = 136.6(2)°$ and $\varphi_2 = 65.4(3)°$, $\psi_2 = 20.3(3)°$, respectively, indicating a type II β-turn structure (Table 1). The turn structure is stabilised by $4 \rightarrow 1$ hydrogen bonds between *m*-ABA—NH and Boc-CO with an N9–O2 distance as 3.18(1) Å, slightly shorter than in **I** and **II** (Table 2). The results demonstrate that the incorporation of *m*-NA and *m*-ABA in β-turn is very well tolerated.

Crystal structure analysis shows that peptides **I** and **II** are packed in a similar fashion to form layers of β-sheets (Figures 5 and 6). In each case, six peptide molecules are interconnected by two types of intermolecular hydrogen bonds Xx(1)—CO···NH—Xx(1) and Aib(2)—CO···NH—Aib(2) to complete each circular subunit (Figures 5(a) and 6(a); Table 2). These circular subunits are interconnected to create layers of β-sheets (*ac* plane). The layer structures

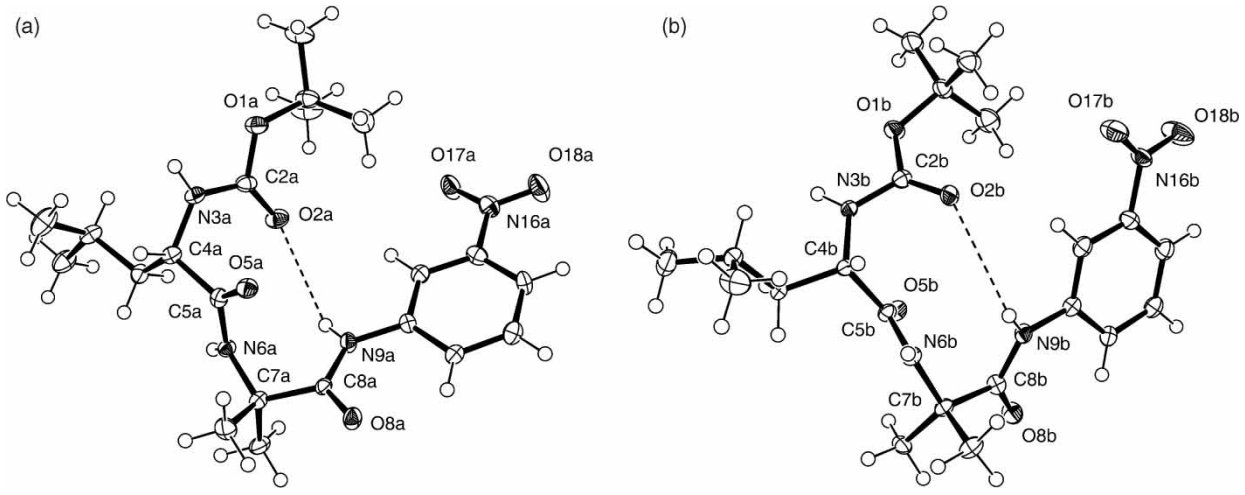

Figure 2. ORTEP diagram of peptide **I** with atom numbering scheme. Thermal ellipsoids are shown at the level of 50% probability.

Table 1. Selected back-bone torsion angles (°) for the peptides **I**–**III**.

Peptide	Residue	ϕ	ψ	ω
IA	Leu (1)	50.3(3)	−132.7(2)	−162.8(2)
	Aib(2)	−61.1(3)	−30.0(3)	−176.5(2)
IB	Leu(1)	−60.6(3)	147.6(2)	170.4(2)
	Aib(2)	58.4(3)	32.1(3)	176.8(2)
II	Phe(1)	−57.9(3)	143.5(2)	172.3(2)
	Aib(2)	70.3(3)	13.2(3)	176.8(2)
III	Pro(1)	−48.4(3)	136.6(2)	171.1(2)
	Aib(2)	65.4(3)	20.3(3)	169.1(2)

of the peptides are further self-assembled along the crystallographic *b*-direction via van der Waals interactions to form higher order supramolecular β-sheet structures (Figures 5(b) and 6(b)). In the case of peptide **III**, the intermolecular hydrogen bond Xx(1)—CO···NH—Xx(1) does not exist as the Pro(1) residue does not provide a suitable proton. The only hydrogen bond Aib(2)—CO···NH—Aib(2) connects the molecules of **III** in the *c*-direction to form semicylindrical structures, which are packed through van der Waals interactions to create layers of β-turns in the *ab* plane (Figure 7).

Interestingly, a previous report shows that the β-turn structure of peptide Boc-Leu-Aib-Phe-OMe, where the *m*NA(3) of peptide **I** has been replaced by Phe, creates a

Table 2. Hydrogen bond parameters for peptides **I**–**III**.

Type	N···O (Å)	H···O (Å)	O···H—N (°)
*Peptide **IA***			
Intramolecular			
N9(A)–H9(A)···O2(A)	3.47(1)	2.76	141
Intermolecular			
N3(A)–H3(A)···O5(B)[a]	2.81(1)	2.01	155
N6(A)–H6(A)···O8(B)[b]	3.01(1)	2.23	152
*Peptide **IB***			
Intramolecular			
N9(B)–H9(B)···O2(B)	3.56	2.95	130
Intermolecular			
N6(B)–H6(B)···O8(A)	2.92(1)	2.11	156
N3(B)–H3(B)···O5(A)[c]	2.93(1)	2.14	154
*Peptide **II***			
Intramolecular			
N9–H9···O2	3.34 (1)	2.59	147
Intermolecular			
N6–H6···O8[d]	2.85(1)	1.99	177
N3–H3···O5[e]	2.90(1)	2.22	136
*Peptide **III***			
Intramolecular			
N9–H9···O2	3.18	2.41	148
Intermolecular			
N6–H6···O8[f]	2.93	2.10	162

Symmetry elements: [a] $1-x$, $0.5+y$, $-z$; [b] $1+x$, y, z; [c] $1-x$, $-0.5+y$, $-z$; [d] $1.5-x$, $-0.5+y$, $-0.5-z$; [e] $2-x$, $1-y$, $-z$; [f] $x-1$, y, z.

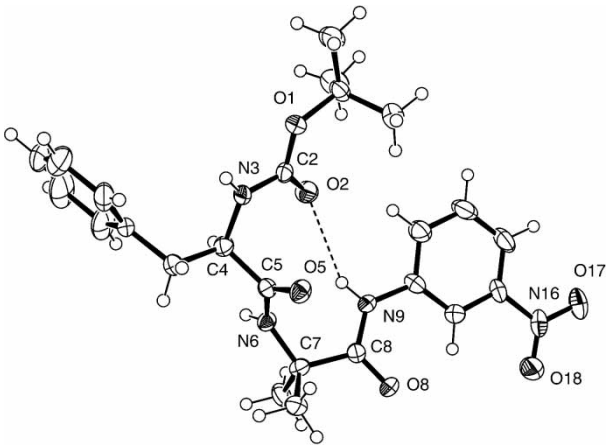

Figure 3. ORTEP diagram of peptide **II** with atom numbering scheme. Thermal ellipsoids are shown at the level of 50% probability.

supramolecular helical structure (*16*). Again, the β-turn structure of peptide Boc-Phe-Aib-Leu-OMe, where the *m*NA(3) of peptide **II** has been replaced by Leu, forms a supramolecular assembly different from β-sheet (*22*). This result indicates that the flat extended conformation of *m*-NA and *m*-ABA in the β-turn structures of peptides **I**–**III** helps to create a β-sheet-like structure through molecular self-assembly.

Peptide conformations in solution

In order to investigate the existence of intramolecular hydrogen bonds and peptide conformations in the solution phase, the solvent dependence of the NH chemical shifts was examined by NMR titrations (*28*, *29*). In this experiment, a solution of peptide **I** in non-polar $CDCl_3$ (10 mM in 0.5 ml) was gradually titrated against polar

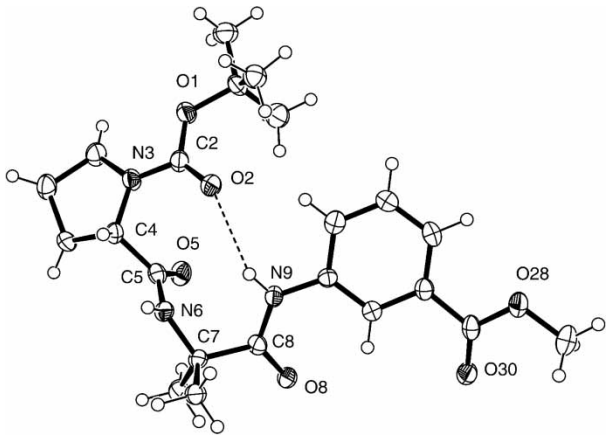

Figure 4. ORTEP diagram of peptide **III** with atom numbering scheme. Thermal ellipsoids are shown at the level of 50% probability.

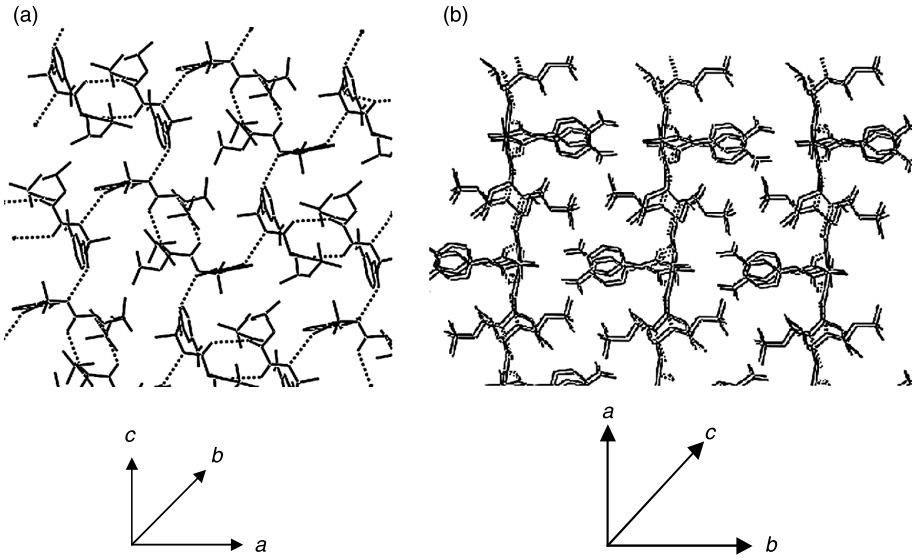

Figure 5. Packing pattern of peptide **I** showing (a) the formation of β-sheet layer in the *ac* plane. Only intermolecular hydrogen bonds are shown with dotted lines. (b) The formation of supramolecular β-sheet through the higher order self-assembly of layers in the *b*-direction.

$(CD_3)_2SO$ and the changes in the chemical shifts of NHs were recorded by ^1H NMR (Figure 8). The solvent titration shows that by increasing the percentage of $(CD_3)_2SO$ in $CDCl_3$ from 0 to 8% (v/v), the net change in the chemical shift ($\Delta\delta$) values for Leu(1)—NH, Aib(2)—NH and *m*NA(3)—NH are 1.00, 0.90 and 0.00 ppm, respectively (Figure 8). The result indicates that Leu(1)—NH and Aib(2)—NH are free and that *m*NA(3)—NH is intramolecularly hydrogen bonded. This corresponds to a β-turn structure in which *m*NA(3)—NH forms a $4 \rightarrow 1$ intramolecular hydrogen bond with Boc-CO as it is observed in the crystal structure (Figure 2). The CD spectra of peptide **I** in methanol at 25°C displays a strong positive ellipticity in the far-UV region with a distinct maxima at 201 nm (Figure 9), which indicates the presence of a β-turn structure (*18*, *30*).

In a similar experiment with peptide **II**, the net changes in the chemical shift ($\Delta\delta$) values for Phe(1)—NH, Aib(2)—NH and *m*NA(3)—NH are found to be 1.10, 0.84 and 0.00 ppm, respectively (Figure 10), thus implying that Phe(1)—NH and Aib(2)—NH are free and *m*NA(3)—NH is intramolecularly hydrogen bonded,

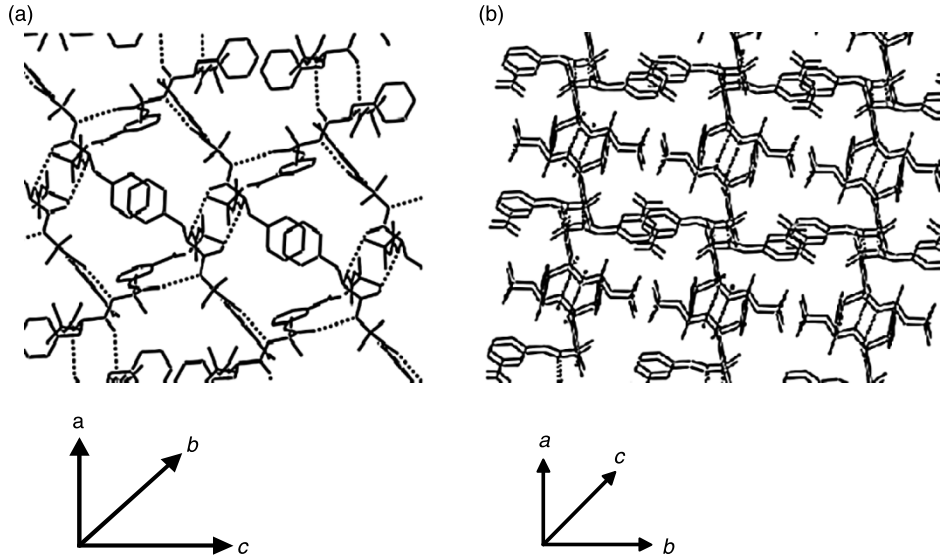

Figure 6. Packing pattern of peptide **II** showing (a) the formation of β-sheet layer in the *ac* plane. Only intermolecular hydrogen bonds are shown with dotted lines. (b) The formation of supramolecular β-sheet through the higher order self-assembly of layers in the *b*-direction.

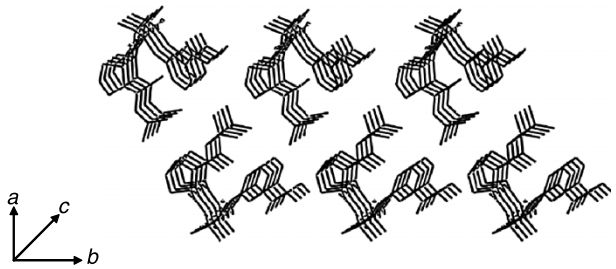

Figure 7. Packing pattern of peptide **III** showing the formation of semicylindrical structures in the *c*-direction. The cylindrical structures are packed through van der Waals interactions to form layers of β-turns in the *ab* plane.

indicating a β-turn conformation similar to the crystal structure (Figure 3). The CD spectrum of peptide **II** in methanol shows a positive ellipticity in the far-UV region with distinct double maxima at 207 and 218 nm, suggesting the presence of a turn structure (Figure 9) (*18*, *30*). The solvent dependence of the NH chemical shifts, which is demonstrated in this $CDCl_3$-$(CD_3)_2SO$ titration experiment, indicates that Aib(2)—NH is free and *m*-ABA(3)—NH is hydrogen bonded in peptide **III** with $\Delta\delta$ values as 0.53 and −0.32, respectively, indicating a β-turn structure (Figure 11). A positive ellipticity with a maxima at 193 nm is observed in the CD spectra of **III** in methanol (Figure 12), indicating the population of β-turn structure. Therefore, the results of solvent-dependent NMR titrations and CD spectroscopy strongly favour the conclusion that the peptides **I**–**III** are folded into β-turn structures in the solution phase.

Morphological studies

Schneider et al. (*31*) have reported the formation of flat fibril laminates through β-sheet-mediated self-assembly

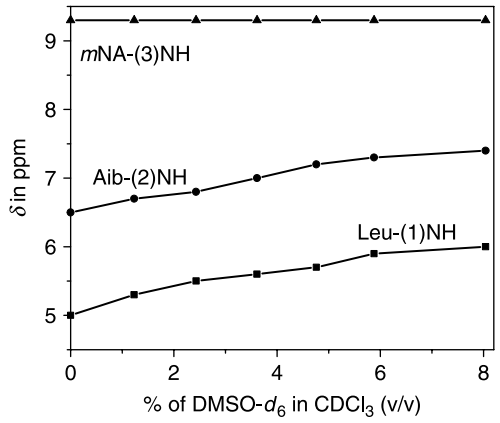

Figure 8. NMR solvent titration curve for NH protons in peptide **I**.

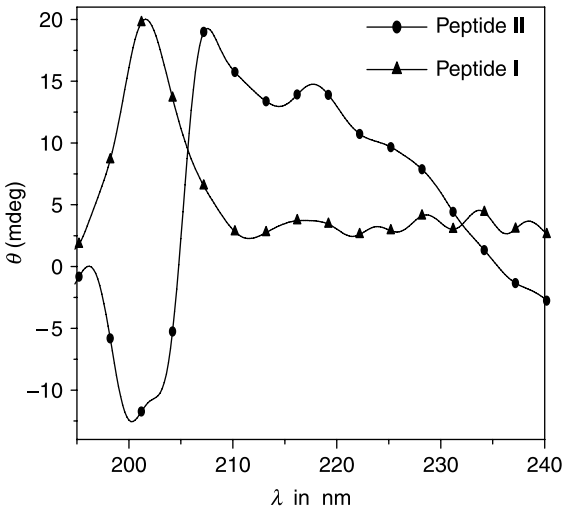

Figure 9. CD curves of peptides **I** and **II** in methanol (1.5 mM).

of peptide with central Pro–Pro fragment. The quasi-crystalline structures of flat and non-twisted morphology are useful for specific nano-applications. Various attempts to fabricate these types of structures using amyloid proteins, peptides and viruses have been reported (*32*–*38*). Therefore, we became interested in exploring the possibility of fibril formation in peptides **I**–**III**. FE-SEM images of the dried fibrous material of peptides **I**–**III** grown slowly from acetone clearly demonstrate that the aggregates in the solid state are bunches of fibrillar structures of flat morphology (Figure 13(a)–(c)). The TEM studies also reveal that the peptides **I**–**III** can form fibrillar structures in the solid state (Figure 14(a)–(c)). The fibrillar structures are formed through β-sheet-mediated self-assembly of the preorganised β-turn building blocks.

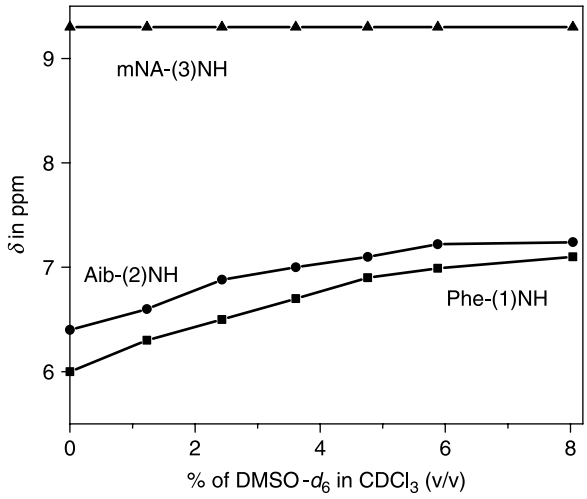

Figure 10. NMR solvent titration curve for NH protons in peptide **II**.

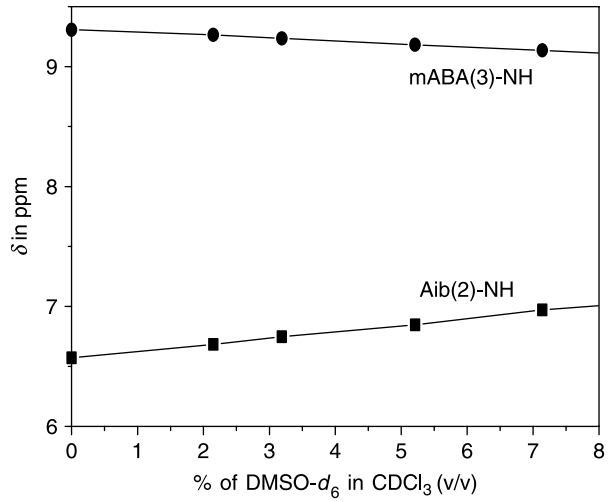

Figure 11. NMR solvent titration curve for NH protons in peptide **III**.

Conclusions

The present studies show that the incorporation of *m*-NA and *m*-ABA in β-turns of acyclic tripeptides is very well tolerated. The β-turn structures generated from the peptides **I**–**III** are found to be quite stable and exist both in the solid state and in solution. The β-turn structures incorporating flat aromatic rings in the backbone such as in peptides **I**–**III** show a high tendency to form supramolecular β-sheets through molecular self-assembly. It has been shown that these preorganised β-turn building blocks generate flat fibrillar structures through β-sheet-mediated self-assembly. The importance of π–π interactions in the formation of amyloid fibrils has also been documented previously (*39*).

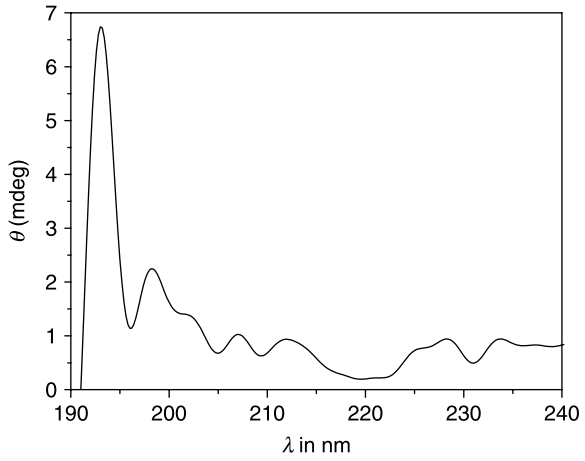

Figure 12. CD curve of peptide **III** in methanol (1.5 mM).

Experimental

Synthesis of the peptides

The peptides were synthesised by conventional solution-phase methods. The Boc group was used for N-terminal protection and the C-terminus was protected as methyl ester. Couplings were mediated by dicyclohexylcarbodiimide (DCC) and 1-hydroxybenzotriazol (HOBT). All intermediates were characterised by thin-layer chromatography (TLC) on silica gel and used without further purification. Final peptides were purified by column chromatography using silica gel (100–200 mesh) as the stationary phase. Ethyl acetate and petroleum ether mixture were used as the eluent. The reported peptides **I**–**III** were fully characterised by X-ray crystallography and NMR studies.

Synthesis of the peptide I, Boc-Leu-Aib-m-NA

Peptide Boc-Leu-Aib-OH (*20*) (1.00 g, 3.16 mmol) was dissolved in 5 ml of dimethylformamide (DMF). *m*-NA (0.87 g, 6.32 mmol) was added to the former solution in ice-cold condition followed by addition of DCC (0.98 g, 4.74 mmol) and HOBT (0.43 g, 3.16 mmol). The reaction mixture was stirred at room temperature for 2 days. The precipitated dicyclohexyl urea (DCU) was filtered. The organic layer was washed with 1 N HCl (3 × 30 ml), brine, 1 M Na_2CO_3 solution (3 × 30 ml) and again with brine. The solvent was then dried over anhydrous Na_2SO_4 and evaporated *in vacuo* giving a white solid. Purification was done using silica gel as the stationary phase and ethyl acetate–petroleum ether mixture (1:4) as the eluent. Single crystals were grown from acetone by slow evaporation and were stable at room temperature. Yield: 1.2 g (88%); mp = 190–192°C; $[\alpha]_{589}^{20} = -20°$ ($c = 0.10$ g per 100 ml; CH_3OH); Anal. calcd for $C_{21}H_{32}N_4O_6$ (436.50): C, 57.78; H, 7.39; N, 12.84. Found: C, 57.82; H, 7.43; N, 12.87%; IR (KBr): 3754.4, 3340.8, 3267.7, 2956.5, 1684.4 and 1528.9 cm^{-1}; ^1H NMR 300 MHz ($CDCl_3$, δ ppm): 0.88–0.99 ($C^{\delta}H$ of Leu(1), 6H, m), 1.48–1.65 (C^{β} and C^{γ} of Leu(1), 3H, m), 1.62 (Boc-CH_3 s, 9H, s), 1.65 ($C^{\beta}H$ of Aib(2), 6H, s), 3.92 ($C^{\alpha}H$ of Leu(1), 1H, m), 4.97 (Leu(1)—NH, 1H, d, $J = 3.3$ Hz), 6.43 (Aib(2)—NH, 1H, s), 7.91 (H_c *m*-NA(3), 1H, dd, $J = 3$ Hz), 7.93 (H_b *m*-NA(3), 1H, dd, $J = 3$ Hz), 8.22 (H_d *m*-NA(3), 1H, d, $J = 7.5$ Hz), 8.56 (H_a *m*-NA(3), 1H, t, $J = 4.2$ Hz) and 9.30 (*m*-NA(3)—NH, 1H, s); ^{13}C NMR 75 MHz ($CDCl_3$, δ ppm): 172.8, 171.6, 156.56, 144.81, 143.23, 124.75, 119.50, 81.40, 58.14, 54.76, 40.12, 28.25, 26.08, 25.10, 24.89, 22.88 and 21.75.

Synthesis of the peptide II, Boc-Phe-Aib-m-NA

Peptide Boc-Phe-Aib-OH (*19*) (0.45 g, 1.28 mmol) was dissolved in 5 ml of DMF. *m*-NA (0.35 g, 2.56 mmol) was

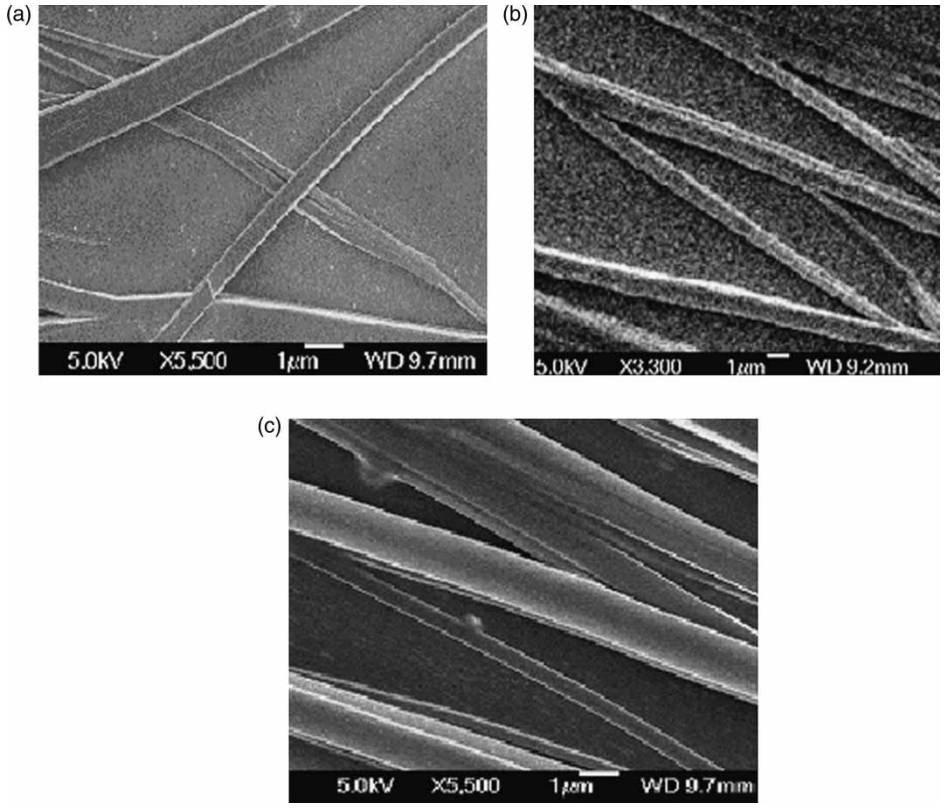

Figure 13. FE-SEM images of (a) peptide **I**, (b) peptide **II** and (c) peptide **III** showing the formation of fibrillar structures of flat morphology in the solid state. The fibrous materials of the peptides were grown slowly from acetone, dried and gold coated.

added to the former solution in ice-cold condition followed by addition of DCC (0.39 g, 1.92 mmol) and HOBT (0.17 g, 1.28 mmol). The reaction mixture was stirred at room temperature for 2 days. The precipitated DCU was filtered. The organic layer was washed with 1 N HCl (3 × 30 ml), brine, 1 M Na_2CO_3 solution (3 × 30 ml) and again with brine. The solvent was then dried over anhydrous Na_2SO_4 and evaporated *in vacuo* giving a white solid. Purification was done using silica gel as the stationary phase and ethyl acetate–petroleum ether mixture (1:4) as the eluent. Single crystals were grown from acetone by slow evaporation and were stable at room temperature. Yield: 0.55 g (92%); mp = 170°C; $[\alpha]_{589}^{20} = -26°$ ($c = 0.10$ g per 100 ml; CH_3OH); Anal. calcd for $C_{24}H_{30}N_4O_6$ (470.51): C, 61.26; H, 6.42; N, 11.91. Found: C, 61.32; H, 6.51; N, 11.97%; IR (KBr): 3753.8, 3324.3, 3407.5, 2980.7, 1674.7 and 1533 cm^{-1}; ^1H NMR 300 MHz ($CDCl_3$, δ ppm): 1.46 and 1.51 ($C^{\beta}H$ of Aib(2), 6H, s), 1.58 (Boc-CH_3 s, 9H, s), 3.06 ($C^{\beta}H$ of Phe(1), 2H, m), 4.11 ($C^{\alpha}H$ of Phe(1), 1H, m), 4.98 (Phe(1)—NH, 1H, d, $J = 3.3$ Hz), 6.08 (Aib(2)—NH, 1H, s), 7.18–7.45 (phenyl ring protons), 7.87 (H_c *m*-NA(3), 1H, dd, $J = 3$ Hz), 7.90 (H_b *m*-NA(3), 1H, dd, $J = 3$ Hz), 8.17 (H_d *m*-NA(3), 1H, d, $J = 7.8$ Hz), 8.51 (H_a *m*-NA(3), 1H, m) and 9.30 (*m*NA(3)—NH, 1H, s); ^{13}C NMR 75 MHz ($CDCl_3$, δ ppm): 172.66, 170.98, 156.44, 148.45, 139.93, 135.91, 129.43, 129.17, 128.99, 127.44, 125.69, 118.28, 114.89, 81.59, 57.99, 57.45, 37.09, 28.15, 25.69 and 25.25.

Synthesis of the peptide III, Boc-Pro-Aib-mABA-OMe

*Boc-Pro-Aib-OMe (**I**)*

Boc-Pro-OH (2.0 g, 9.30 mmol) was dissolved in a mixture of dichloromethane (DCM, 6 ml) and DMF (2 ml). Aib-OMe obtained from its hydrochloride (2.85 g, 18.6 mmol) was added to the former solution followed by addition of DCC (2.87 g, 13.95 mmol) in ice-cold condition. The reaction mixture was stirred at room temperature for 1 day. The precipitated DCU was filtered. The organic layer was washed with 1 N HCl (3 × 30 ml), brine, 1 M Na_2CO_3 solution (3 × 30 ml) and then again with brine. The solvent was dried over anhydrous Na_2SO_4 and evaporated *in vacuo*, giving a light yellow gum. Yield: 2.5 g (86%).

*Boc-Pro-Aib-OH (**II**)*

Peptide **I** (2.5 g, 7.96 mmol) was dissolved in methanol (20 ml) and 2 N NaOH (10 ml) was added to it. The reaction mixture was stirred for 1 day at room temperature. The progress of the reaction was monitored by TLC. After completion of the reaction, the methanol was evaporated.

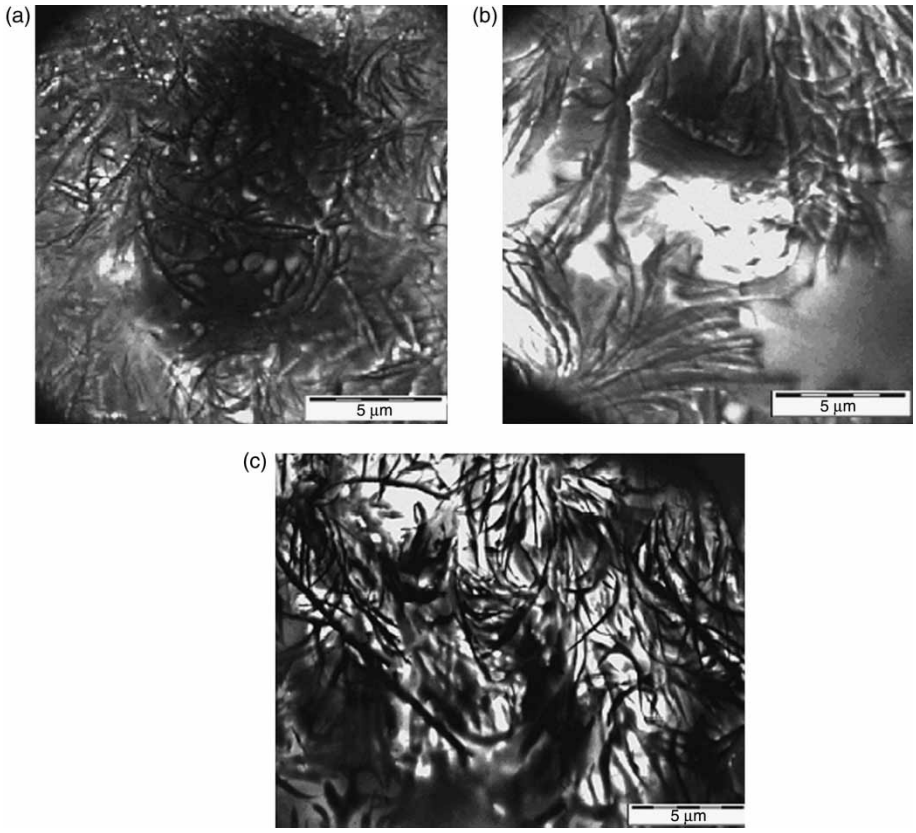

Figure 14. TEM images of (a) peptide **I**, (b) peptide **II** and (c) peptide **III** showing the formation of fibrillar morphology in the solid state. The transmission electron microscopic studies of all the peptides were carried out using a small amount of the solution (1×10^{-3} M) of the corresponding peptides on carbon-coated copper grids (300 mesh) by slow evaporation.

The residue was diluted with water and washed with diethyl ether. The aqueous layer was cooled on ice, neutralised by using 2 N HCl and extracted with ethyl acetate. The solvent was evaporated *in vacuo* to give a waxy white coloured solid. Yield: 2.1 g (88%).

*Boc-Pro-Aib-mABA-OMe (**III**)*

Peptide **II** (2.1 g, 7.00 mmol) was dissolved in DCM (5 ml). *m*ABA-OMe obtained from its hydrochloride (2.62 g, 14 mmol) was added to former solution, followed by addition of DCC (2.16 g, 10.5 mmol) in ice-cold condition. The reaction mixture was stirred at room temperature for 2 days. The precipitated DCU was filtered. The organic layer was washed with 1 N HCl (3 × 30 ml), brine, 1 M Na_2CO_3 solution (3 × 30 ml) and then again with brine. The solvent was then dried over anhydrous Na_2SO_4 and evaporated *in vacuo*, to give a white solid compound. Purification was done using silica gel as the stationary phase and ethyl acetate–petroleum ether mixture (1:4) as the eluent. Single crystals were grown from acetone by slow evaporation and were stable at room temperature. Yield: 2.6 g (86%); mp = 158°C; $[\alpha]_{589}^{20} = -19°$ ($c = 0.10$ g per 100 ml; CH_3OH); Anal. calcd for $C_{22}H_{31}N_3O_6$ (433.49): C, 60.95; H, 7.20; N, 9.69%. Found: C, 61.02; H, 7.25; N, 9.61; IR (KBr): 3754.2, 3356.8, 3294.4, 2978.9, 1689.4 and 1544.4 cm^{-1}; ^{1}H NMR 300 MHz ($CDCl_3$, δ ppm): 1.48 (Boc-CH_3 s, 9H, s), 1.58 ($C^{\beta}H$ of Aib(2), 6H, s), 1.90 ($C^{\delta}H$ of Pro(1), 2H, m), 2.13 ($C^{\beta}H$ of Pro(1), 2H, m), 3.48 ($C^{\gamma}H$ of Pro(1), 2H, m), 3.88 (—OCH_3, 3H, s), 4.14 ($C^{\alpha}H$ of Pro(1), 1H, m), 6.57 (Aib(2)—NH, 1H, s), 7.31 (H_c *m*-ABA(3), 1H, t, $J = 7.8$ Hz), 7.74 (H_b *m*-ABA(3), 1H, d, $J = 7.8$ Hz), 8.00 (H_d *m*-ABA(3), 1H, d, $J = 7.5$ Hz), 8.26 (H_a *m*-ABA(3), 1H, broad s) and 9.30 (*m*ABA(3)—NH, 1H, s); ^{13}C NMR 75 MHz ($CDCl_3$, δ ppm): 172.55, 168.80, 166.88, 138.88, 130.59, 128.73, 124.97, 124.70, 121.20, 81.13, 61.30, 57.97, 51.99, 47.33, 29.26, 28.27, 26.36, 25.24 and 24.64.

FT-IR spectroscopy

The IR spectra were examined using a Perkin-Elmer-782 model spectrophotometer. The solid-state FT-IR measurements were performed using the KBr disc technique.

NMR experiments

All the ^{1}H and ^{13}C NMR studies were recorded on a Bruker Avance 300 model spectrometer operating at 300 and

75 MHz, respectively. The peptide concentrations were 10 mM in $CDCl_3$ for ^1H NMR and 40 mM in $CDCl_3$ for ^{13}C NMR. Solvent titration experiments were carried out at a concentration of 10 mM in $CDCl_3$ with gradual addition of DMSO-d_6 from 0 to 8% (v/v) approximately.

Circular dichroism spectroscopy

Solutions of peptides **I**–**III** in MeOH (1.5 mM as the final concentration) were used for obtaining the spectra. Far-UV CD measurements were recorded at 25°C with a 0.5 s averaging time, a scan speed of 50 nm/min, using a JASCO spectropolarimeter (J 720 model) equipped with a 0.1 cm path-length cuvette. The measurements were taken at 0.2 nm wavelength intervals, 2.0 nm spectral bandwidth and five sequential scans were recorded for each sample.

Field emission scanning electron microscopic study

The morphology of peptides **I**–**III** was investigated using FE-SEM. For this study, fibrous materials (fibrous materials of peptides **I**–**III** were slowly grown from acetone) were dried and gold coated. The micrographs were taken using a FE-SEM apparatus (JEOL JSM-6700F).

Transmission electron microscopy

The morphology of the reported peptides **I**–**III** was investigated using TEM. The solutions of the peptides (1×10^{-3} M) were prepared in acetone. The transmission electron microscopic studies of all the peptides were carried out using a small amount of the solution of the corresponding peptides on carbon-coated copper grids (300 mesh) by slow evaporation and allowed to dry in vacuum at 30°C for 2 days. Images were taken at a voltage of 80 kV. TEM was carried out by a JEM-2010 electron microscope and a FEI (Tecnai spirit) instrument.

Single crystal X-ray diffraction study

Crystal data and refinement details are given in Table 3. Diffraction data for the three peptides **I**, **II** and **III** were obtained with Mo Kα radiation at 150 K using the Oxford Diffraction X-Calibur CCD System. The crystals were positioned at 50 mm from the CCD. Three hundred and twenty-one frames were measured with a counting time of 10 s. Data analyses were carried out with the Crysalis program (*40*). The structures were solved using direct methods using the SHELX97 program (*41*). The non-hydrogen atoms were refined with anisotropic thermal parameters. The hydrogen atoms bonded to carbon were included in geometric positions and given thermal parameters equivalent to 1.2 times those of the atom to which they were attached. Peptides **I** and **III** crystallised in non-centrosymmetric space groups and their absolute structure could not be determined in the X-ray analysis. In both structures, coordinates were chosen to conform to C(4) having the same *S* chirality as the Leu starting material. The structure of peptide **I** contained two

Table 3. Crystallographic refinement details for peptides **I**–**III**.

	Peptide **I**	Peptide **II**	Peptide **III**
Crystal colour	Colourless	Colourless	Colourless
Chemical formula	$C_{21}H_{32}N_4O_6$	$C_{24}H_{30}N_4O_6$	$C_{22}H_{28}N_3O_6$
Formula weight (g)	436.51	470.51	430.3.47
Crystal system	Monoclinic	Monoclinic	Monoclinic
Space group	$P2_1$	$P2_1/n$	$P2_1$
Z	4	4	2
a (Å)	10.8030(4)	14.7371(8)	6.0300(6)
b (Å)	18.6839(5)	11.1049(5)	11.2038(18)
c (Å)	11.7419(4)	15.1024(7)	16.783(3)
β (°)	104.546(4)	92.702(4)	97.546(11)
V (Å^3)	2294.04(13)	2468.8(2)	1124.0(3)
Temperature (K)	150	150	150
μ (Mo Kα) (mm^{-1})	0.093	0.092	0.093
Collected reflections	15,986	15,535	7290
Unique reflections	9530	6986	5710
Reflections $I > 2\sigma(I)$	7429	2887	3665
No. of parameters	573	312	286
R(int)	0.0262	0.0739	0.0274
Goodness-of-fit	0.756	0.969	0.961
R_1, $wR2$ [$I > 2\sigma(I)$]	0.0487, 0.1398	0.0801, 0.1273	0.0527, 0.1207
R_1, $wR2$ [all data]	0.0661, 0.1566	0.2064, 0.1674	0.0810, 0.1358
Max., min. electron density (e/Å^3)	0.264, −0.272	0.228, −0.300	0.406, −0.312

molecules in the asymmetric unit with equivalent chirality at C(4). However, peptide **II** crystallised in a centrosymmetric space group, and it can be assumed that epimerisation must have occurred during the synthesis. Crystallographic details have been deposited at the Cambridge Crystallographic Data Centre; reference CCDC Nos are 701495–701497.

Acknowledgements

We thank EPSRC and the University of Reading, UK for funds for Oxford Diffraction X-Calibur CCD diffractometer. S.K. and A.D. would like to thank CSIR, New Delhi, India, for providing Senior Research Fellowship. P.K. thanks UGC, New Delhi for providing Project Fellowship. The financial assistance of UGC, New Delhi is acknowledged (Major Research Project No. 32-190/2006 (SR)).

References

(1) Maji, S.K.; Banerjee, A.; Drew, M.G.B.; Halder, D.; Banerjee, A. *Tetrahedron Lett.* **2002**, *43*, 6759–6762.
(2) Halder, D.; Maji, S.K.; Drew, M.G.B.; Banerjee, A. *Tetrahedron Lett.* **2002**, *43*, 5465–5468.
(3) Maji, S.K.; Drew, M.G.B.; Banerjee, A. *Chem. Commun.* **2001**, *19*, 1946–1947.
(4) Vauthey, S.; Santoso, S.; Gong, H.; Watson, N.; Zhang, S. *Proc. Natl Acad. Sci. USA* **2002**, *99*, 5355–5360.
(5) Rathore, O.; Sogah, D.Y. *J. Am. Chem. Soc.* **2001**, *123*, 5231–5239.
(6) Caplan, M.R.; Moore, P.N.; Zhang, S.; Kamm, R.D.; Lauffenburger, D.A. *Biomacromolecules* **2000**, *1*, 627–631.
(7) Krejchi, M.T.; Atkins, E.D.T.; Waddon, A.J.; Fournier, M.J.; Mason, T.L.; Tirrel, D.A. *Science* **1994**, *265*, 1427–1432.
(8) Wang, W.; Hecht, M.H. *Proc. Natl Acad. Sci. USA* **2002**, *99*, 2760–2765.
(9) Antzutkin, O.N.; Balbach, J.J.; Leapman, R.D.; Rizzo, N.W.; Reed, J.; Tycko, R. *Proc. Natl Acad. Sci. USA* **2000**, *97*, 13045–13050.
(10) Tjernberg, L.O.; Callway, D.J.E.; Tjernberg, A.; Hahne, S.; Lilliehöök, C.; Terenius, L.; Thyberg, J.; Nordsted, C. *J. Biol. Chem.* **1999**, *274*, 12619–12625.
(11) Benzinger, T.L.S.; Gregory, D.M.; Burkoth, T.S.; Miller-Auer, H.; Lynn, D.G.; Botto, R.E.; Maredith, S.C. *Proc. Natl Acad. Sci. USA* **1998**, *95*, 13407–13412.
(12) Dutt, A.; Drew, M.G.B.; Pramanik, A. *Org. Biomol. Chem.* **2005**, *3*, 2250–2254.
(13) Kundu, S.K.; Majumdar, P.A.; Das, A.K.; Bertolasi, V.; Pramanik, A. *J. Chem. Soc., Perkin Trans. 2* **2002**, 1602–1604.
(14) Maji, S.K.; Haldar, D.; Drew, M.G.B.; Banerjee, A.; Das, A.K.; Banerjee, A. *Tetrahedron* **2004**, *60*, 3251–3259.
(15) Banerjee, A.; Maji, S.K.; Drew, M.G.B.; Haldar, D.; Banerjee, A. *Tetrahedron Lett.* **2003**, *44*, 335–339.
(16) Halder, D.; Maji, S.K.; Sheldrick, W.S.; Banerjee, A. *Tetrahedron Lett.* **2002**, *43*, 2653–2656.
(17) Lashuel, H.A.; LaBrenz, S.R.; Woo, L.; Serpell, L.C.; Kelly, J.W. *J. Am. Chem. Soc.* **2000**, *122*, 5262–5277.
(18) Dutt, A.; Dutta, A.; Mondal, R.; Spencer, E.C.; Howard, J.A.K.; Pramanik, A. *Tetrahedron* **2007**, *63*, 10282–10289.
(19) Halder, D.; Drew, M.G.B.; Banerjee, A. *Tetrahedron* **2007**, *63*, 5561–5566.
(20) Dutt, A.; Drew, M.G.B.; Pramanik, A. *Tetrahedron* **2005**, *61*, 11163–11167.
(21) Das, A.K.; Banerjee, A.; Drew, M.G.B.; Ray, S.; Haldar, D.; Banerjee, A. *Tetrahedron* **2005**, *61*, 5027–5036.
(22) Dutt, A.; Frohlick, R.; Pramanik, A. *Org. Biomol. Chem.* **2005**, *3*, 661–665.
(23) Banerjee, A.; Maji, S.K.; Drew, M.G.B.; Haldar, D.; Banerjee, A. *Tetrahedron Lett.* **2003**, *44*, 6741–6744.
(24) Maji, S.K.; Malik, S.; Drew, M.G.B.; Nandi, A.K.; Banerjee, A. *Tetrahedron Lett.* **2003**, *44*, 4103–4107.
(25) Lee, H.B.; Zaccaro, M.C.; Pattarawarapan, M.; Roy, S.; Saragovi, H.B.; Burgess, K. *J. Org. Chem.* **2004**, *69*, 701–713.
(26) Venkatachalam, C.M. *Biopolymers* **1968**, *6*, 1425–1436.
(27) Nicholson, L.K.; Yamazaki, T.; Torchia, D.A.; Grzesiek, S.; Bax, A.; Stahl, S.J.; Kaufman, J.D.; Wingfield, P.T.; Lam, P.Y.S.; Jadav, P.K.; Hodge, C.N.; Domaill, P.J.; Chang, C.-H. *Nat. Struct. Biol.* **1995**, *2*, 274–280.
(28) Banerjee, A.; Raghothama, S.; Balaram, P. *J. Chem. Soc. Perkin Trans. 2* **1997**, 2087–2094.
(29) Karle, I.L.; Banerjee, A.; Bhattacharya, S.; Balaram, P. *Biopolymers* **1996**, *38*, 515–526.
(30) Prasad, S.; Rao, R.B.; Balaram, P. *Biopolymers* **1994**, *35*, 11–20.
(31) Lamm, M.S.; Rajagopal, K.; Schneider, J.P.; Pochan, D.J. *J. Am. Chem. Soc.* **2005**, *127*, 16692–16700.
(32) Sone, E.D.; Stupp, S.I. *J. Am. Chem. Soc.* **2004**, *126*, 12756–12757.
(33) Meegan, J.E.; Aggeli, A.; Boden, N.; Brydson, R.; Brown, A.P.; Carrick, L.; Brough, A.R.; Hussain, A.; Ansell, R.J. *Adv. Funct. Mater.* **2004**, *14*, 31–37.
(34) Mao, C.; Flynn, C.E.; Hayhurst, A.; Sweeney, R.; Qi, J.; Georgiou, G.; Iverson, B.; Belcher, A.M. *Proc. Natl Acad. Sci. USA* **2003**, *100*, 6946–6951.
(35) Scheibel, T.; Parthasarathy, R.; Sawicki, G.; Lin, X.M.; Jaeger, H.; Lindquist, S.L. *Proc. Natl Acad. Sci. USA* **2003**, *100*, 4527–4532.
(36) McMillan, R.A.; Paavola, C.D.; Howard, J.; Chan, S.L.; Zaluzec, N.J.; Trent, J.D. *Nat. Mater.* **2002**, *1*, 247–252.
(37) Hartgerink, J.D.; Beniash, E.; Stupp, S.I. *Science* **2001**, *294*, 1684–1688.
(38) Shenton, W.; Douglas, T.; Young, M.; Stubbs, G.; Mann, S. *Adv. Mater.* **1999**, *11*, 253–256.
(39) Gazit, E. *J. FASEB* **2002**, *16*, 77–83.
(40) Crysalis, v1; Oxford Diffraction Ltd, Oxford, 2005.
(41) Sheldrick, G.M. SHELXS-97 and SHELXL-97, Programs for Crystal Structure solution and determination. University of Göttingen: Göttingen, 1997.